

# RF-thermal-structural-RF coupled analysis on a travelling wave disk-loaded accelerating structure

PEI Shi-Lun(裴士伦)<sup>1)</sup> CHI Yun-Long(池云龙) ZHANG Jing-Ru(张敬如)  
HOU Mi(侯汭) LI Xiao-Ping(李小平)

Institute of High Energy Physics, Chinese Academy of Sciences, Beijing 100049, China

**Abstract:** The travelling wave (TW) disk-loaded accelerating structure is one of the key components in normal conducting (NC) linear accelerators, and has been studied for many years. In the design process, usually after the dimensions of each cell and the two couplers are finalized, the structure is fabricated and tuned, and then the whole structure RF characteristics are measured by using a vector network analyzer. Before fabrication, the whole structure characteristics (including RF, thermal and structural ones) are less simulated due to the limited capability of currently available computers. In this paper, we described a method for performing RF-thermal-structural-RF coupled analysis on a TW disk-loaded structure using only one PC. In order to validate our method, we first analyzed and compared our RF simulation results on the 3 m long BEPC II structure with the corresponding experimental results, which shows very good consistency. Finally, the RF-thermal-structure-RF coupled analysis results on the 1.35 m long NSC KIPT linac accelerating structure are presented.

**Key words:** RF-thermal-structural-RF coupled analysis, travelling wave, disk-loaded accelerating structure, normal conducting, ANSYS

**PACS:** 41.20.Jb, 44.05.+e, 44.10.+I     **DOI:** 10.1088/1674-1137/36/6/013

## 1 Introduction

An accelerating structure is a device used to boost particle energy. The travelling wave (TW) disk-loaded accelerating structure is mostly used in normal conducting (NC) linear accelerators, such as the BEPC and BEPC II linacs [1, 2]. In the usual design process, the physical dimensions of each cell and the two couplers are determined first, and then the structure is fabricated and tuned. The whole structure RF characteristics are less simulated but measured after the final microwave tuning. This is because of the structural scale (couples of several meters long and centimeters in diameter for S-band) and also computer capability limitations. However, for structures with very high RF input power, thermal and structural effects must be studied before mechanical fabrication, so the travelling wave RF electromagnetic fields in the whole structure need to be calculated first.

Because the characteristics of TW structures with

several tens of cells are mainly decided by the regular cells, we propose a method to use redesigned power couplers with azimuth symmetry to replace the original waveguide ones in finite element analysis (FEA). Then the coupled RF-thermal-structural-RF analysis can be performed by using the multi-physics software package ANSYS [3] with much less computer resources required. In order to prove the validity of our methods, we first simulated the RF characteristics of the BEPC II linac structure, and then compared it with the experimental results, which shows very good consistency, except for a slight difference of the frequency bandwidth. Finally we investigated the RF-thermal-structural-RF effects in the accelerating structure for the NSC KIPT (National Science Center, Kharkov Institute of Physics and Technology, Ukraine) linac [4], which is a cooperative project of the ANL (Argonne National Laboratory, USA) and KIPT. The linac is designed by IHEP, and will be used to drive a neutron source on the basis of sub-critical assembly [5]. Table 1 shows the main specifi-

---

Received 17 August 2011

1) E-mail: peisl@mail.ihep.ac.cn

©2012 Chinese Physical Society and the Institute of High Energy Physics of the Chinese Academy of Sciences and the Institute of Modern Physics of the Chinese Academy of Sciences and IOP Publishing Ltd

Table 1. Main specifications of the TW structures for the BEPC II and KIPT linacs.

	NSC-KIPT	BEPC II
operating frequency/MHz	2856	2856
operating temperature/°C	40.0±0.1	45.0±0.1
number of cells	34 regular cells 2 coupler cells	85 regular cells 2 coupler cells
section length/mm	1260 (36 cells)	3045 (87 cells)
phase advance per cell	$2\pi/3$	$2\pi/3$
cell length/mm	34.989783	34.989783
disk thickness ( $t$ )/mm	5.84	5.84
iris diameter ( $2a$ )/mm	27.887–23.726	26.220–19.093
cell diameter ( $2b$ )/mm	83.968–82.776	83.458–81.762
shunt impedance ( $r_0$ )/(MΩ/m)	51.514–57.052	53.708–63.294
$Q$ factor	13806–13753	13783–13711
group velocity ( $v_g/c$ )	0.02473–0.01415	0.02004–0.0063
filling time/ns	215	823
attenuation parameter/Np	0.1406	0.5383

cations of the TW structures for the BEPC II and KIPT linacs.

## 2 ANSYS simulation methodology

The high frequency, steady-state thermal and structural solver modules in ANSYS can be used to perform the numerical RF-thermal-structural-RF coupled finite element analysis. By using one program for all of the simulations any problems of transferring loads between different types of software were eliminated.

A complete RF-thermal-structural-RF coupled analysis cycle on the TW disk-loaded structure requires 6 steps, as outlined below. Here we assume that the structure is cooled with the water cooling jacket, which surrounds the whole accelerating structure axisymmetrically. Currently, the ANSYS high frequency module has the limitation that only 3D elements can be used. To minimize the CPU time and memory use, an axis-symmetric 3D model with a  $1^\circ$  azimuth angle was created to perform the analysis. Otherwise, the azimuth angle of the model needs to be adjusted correspondingly.

1) With an HF119 high frequency tetrahedral element, modal analysis was performed in the vacuum part of each accelerating cell, the cell diameter  $2b$  was

varied to tune the  $2\pi/3$  mode resonating at the nominal operating frequency (2856 MHz for the BEPC II and KIPT linacs) by fixing the iris diameter  $2a$ . The redesigned axisymmetric vacuum models of the input/output couplers can be defined by using the obtained dimensions of the first/last cells. To minimize the reflection coefficient at the input coupler port to the level of  $10^{-2}$  to  $10^{-3}$ , all of the dimensions shown in Fig. 1 except those related with the middle two cells can be adjusted. Once a flat electric field amplitude distribution along the redesigned coupler's axis is obtained and the phase difference between the middle two cells is  $\sim 120^\circ(2\pi/3)$ , the coupler's dimension can be finalized.

2) Now the vacuum part of the whole structure can be modeled with the obtained cell and coupler dimensions from Step 1. In the meantime, the copper part can also be established with the known dimensions from the mechanical design. Both parts need to be meshed with a common surface interface but different 3D elements (HF119 for vacuum part, while SOLID87 for copper part). A common surface mesh can facilitate the load transfer of the RF wall losses to heat flux loads onto the thermal model surfaces.

3) Harmonic analysis in the vacuum part was carried out with the specified average input power. The two redesigned couplers in Step 1 were defined as the power input and output ports, respectively.

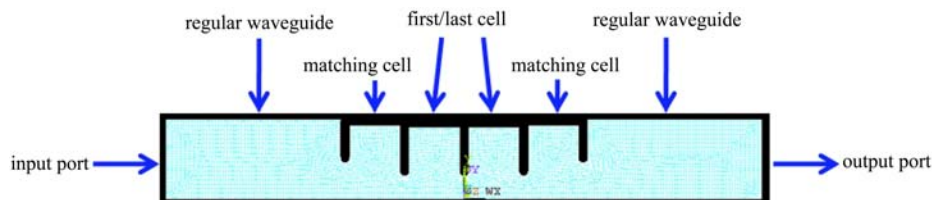


Fig. 1. Schematic of the redesigned input/output couplers.

Impedance boundary condition of copper was applied to the common surface. Using the built-in macro ‘SPARM’ and ‘HFPOWER’, it is possible to calculate the scattering ( $S$ ) parameters and the total time averaged losses. If a harmonic response over a frequency range is performed, the  $S$  parameters at each frequency step for each port will be calculated, the structure’s bandwidth ( $VSWR \leq 1.2$ ) can then be known by checking the  $S_{11}/VSWR$  data.

4) With the method described in Ref. [6], the thermal convection coefficient on the cooling water jacket surface can be calculated by using the empirical formulae [7]. The temperature distribution on the structure wall was calculated after the heat flux and the convection coefficient loads were applied onto the specific surface of the copper volume.

5) By using the built-in macro ‘ETCHG’, thermal element SOLID87 was converted to structural element SOLID187. Then the structure distortion caused by RF heating could be simulated by applying appropriate DOF (degree of freedom) constraints and the thermal results as loads.

6) The displacements from the analysis in Step 5 were added to the geometry of the finite element model created in Step 2 with the ‘UPGEOM’ command. The macro ‘ETCHG’ was issued again to convert the structural element back to the thermal one. By only selecting the vacuum part model and setting the corresponding RF boundaries, the RF characteristics of the deformed structure can be re-calculated.

It is worth to point out that the mesh size consistency in all of the above analysis steps is the key for acquiring the correct simulation results. Only in Steps 1 and 2, the corresponding model dimensions need to be adjusted.

### 3 The BEPC II-linac structure

If we use the real coupler dimensions to simulate

the RF characteristics of the whole BEPC II-linac accelerating structure, at least a 1/2 model (180° azimuth angle) needs to be created, which is impossible to simulate with only one PC. However, with the method proposed in Section 2, only a 1/360 model needs to be established.

Figure 2 shows the 1/360 BEPC II linac structure model. Fig. 3 shows the electric field amplitude distribution along the structure’s axis. The ANSYS result is consistent with the analytical one, which can be calculated with the analytical formulae [8] after obtaining each cell’s RF parameters such as the frequency, quality factor  $Q_0$ , shunt impedance  $R$  and the group velocity  $v_g$ . Usually, the former three ones can be calculated with SUPERFISH [9], and the last one with MAFIA [10].

With  $-34$  dB reflection coefficient at the input port, the ANSYS simulated power attenuation factor to the output port is 0.56 Np (4.85 dB), which is very close to the experimentally measured (0.57 Np) and analytically calculated (0.54 Np) ones.



Fig. 2. The 1/360 model of the BEPC II linac structure.

Figures 4 and 5 show the simulated and experimentally measured VSWR curves, respectively. It can be seen that the simulated bandwidth is  $2858.05 - 2854.5 = 3.55$  MHz, while the measured one is  $2858.42 - 2853.72 = 4.7$  MHz.

Generally speaking, our ANSYS simulation results agree with the experimental ones, except for the 1.15 MHz difference in the bandwidth results.

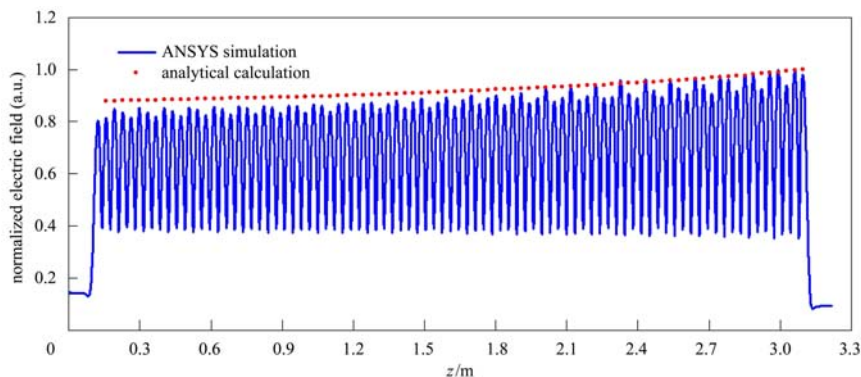


Fig. 3. The electric field amplitude distribution along the structure’s axis of the BEPC II-linac.

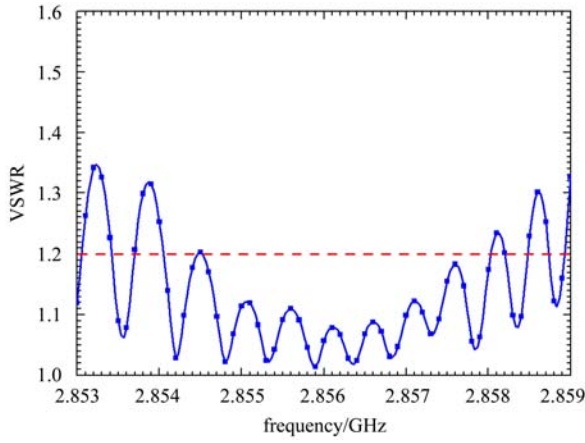


Fig. 4. The ANSYS simulated VSWR curve.

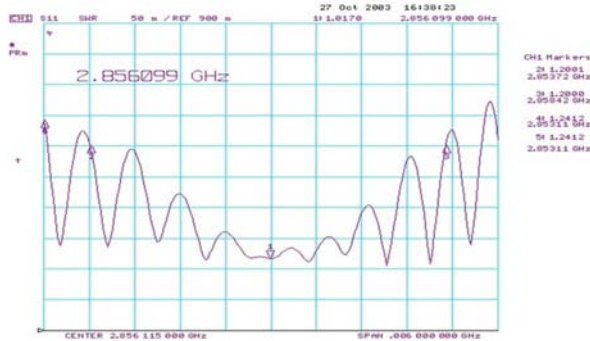


Fig. 5. The measured VSWR curve.

#### 4 The NSC KIPT-linac structure

An electron with very high beam current ( $\sim 600$  mA) will travel through all 10 accelerating structures of the KIPT-linac [4, 5], so very high RF power (20 MW for maximum peak power,  $20 \text{ MW} \times 3 \mu\text{s} \times 625 \text{ Hz} = 37.5 \text{ kW}$  for maximum average power) is needed to compensate the beam loading effect [4, 8], and water jacket cooling is needed to cool the structure sufficiently. Due to the energy extraction of the beam (beam loading), the electric field in the structure for the beam-off case is higher than that for the beam-on case. Since ANSYS cannot simulate the beam loading effect, the RF electric field amplitude and RF heating loss distribution need to be scaled from the beam-off case. The scaling relation can be obtained from the analytical calculation [8].

With the beam-off case, the RF electric field amplitude distribution along the structure's axis is shown in Fig. 6. The attenuation factor simulated by ANSYS is 0.15 Np, while it is 0.14 Np by using the analytical calculation.

The cooling water jacket is an annular water pipe with internal and external diameters of 102 mm and

116 mm. 10 t/h was chosen to be the water flow rate.

When the water cooling temperature is controlled to be  $40^\circ\text{C}$ , the temperature distributions along the structure for both the beam-off and beam-on cases are shown in Fig. 7. The maximum temperature rise is located at the output coupler part when the beam is off, which is due to the highest electromagnetic field. On the contrary, when the beam is on, due to the beam loading effect, the input coupler part will have the highest electric field and maximum temperature rise. For both the beam-off and beam-on cases, the highest temperatures are all located at the iris tips. The maximum temperature differences along the structure are  $\sim 10^\circ\text{C}$  and  $\sim 7^\circ\text{C}$  for both cases.

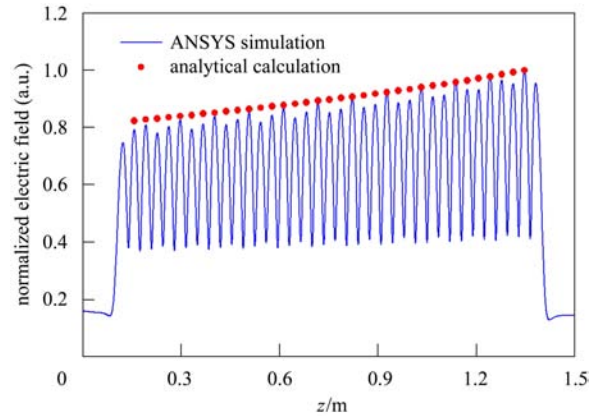


Fig. 6. The electric field amplitude distribution along the structure's axis for the KIPT-linac.

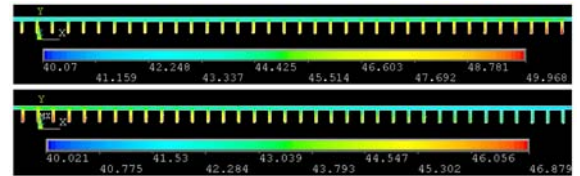


Fig. 7. The temperature distributions along the structure for the beam-off (upper) and on (lower) cases (unit:  $^\circ\text{C}$ ).

If the reference temperature is also set to be  $40^\circ\text{C}$ , the structure deformations for  $40^\circ\text{C}$  cooling water are shown in Figs. 8 and 9. The longitudinal deformation can cause electric field phase shift, while the transversal one is a major source of frequency shift. Here the phase shifts caused by longitudinal deformations are  $\sim 0.72^\circ$  and  $\sim 0.60^\circ$  for the beam-off and beam-on cases, respectively. With the scaling law  $\Delta f / \Delta(2b) = -36 \text{ kHz}/\mu\text{m}$  [11], the frequency shifts caused by the transversal deformations can be roughly calculated to be  $\sim 0.68 \text{ MHz}$  and  $\sim 0.58 \text{ MHz}$  for both cases.

The VSWRs of the accelerating structure versus frequency for both the beam-off and beam-on are

shown in Figs. 10 and 11. The RF heating will cause the VSWR curves to shift downward to lower frequencies by  $\sim 0.6$  MHz and  $\sim 0.5$  MHz for both cases, which are a little bit smaller than the scaling law method estimations. These small differences are due to the fact that the scaling law method calculation is estimated by the largest transversal deformation, while in reality not every cell has that large deformation. The bandwidth of the structure is  $\sim 5.4$  MHz defined by  $VSWR \leq 1.2$ , which is fairly larger than the RF heating caused frequency shift and assures the stable operation of the accelerating structure.

For the KIPT-linac accelerating structure, once the tuning is finished and the water cooling jacket is mounted, it can no longer be tuned. At this time, the only way to suppress the structure RF characteristics deterioration caused by the RF heating is to adjust and optimize the cooling water temperature.

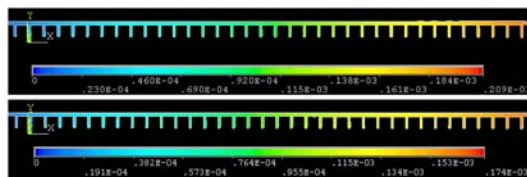


Fig. 8. The longitudinal deformations along the structure for the beam-off (upper) and on (lower) cases (unit: m).

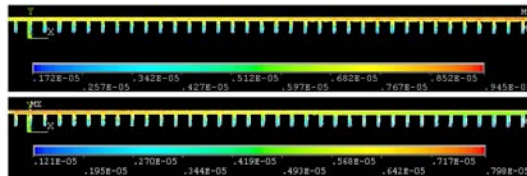


Fig. 9. The transversal deformations along the structure for the beam-off (upper) and on (lower) cases (unit: m).

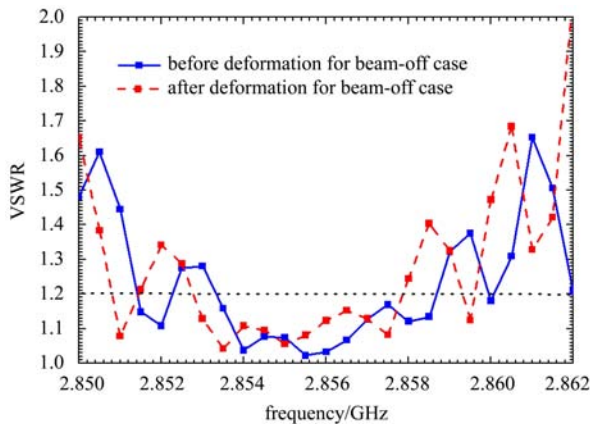


Fig. 10. The VSWR curve for the beam-off case.

Figures 12 to 16 show the structure characteristic variations (such as the maximum temperature,

the longitudinal deformation, the total phase shift, the maximum transversal deformation, the frequency shift, etc.) at different cooling water temperatures for both the beam-off and beam-on cases. It can be seen that one can lower the electric field phase shift and

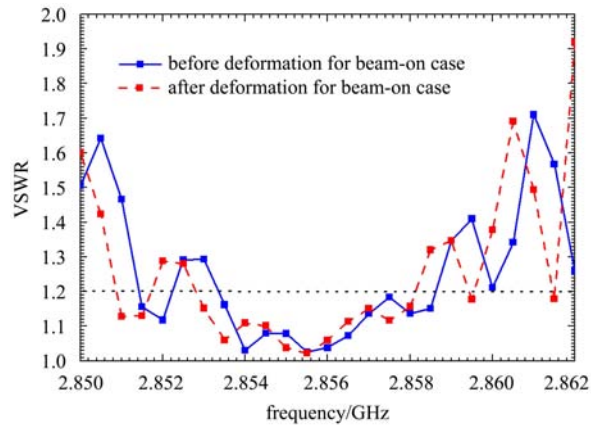


Fig. 11. The VSWR curve for the beam-on case.

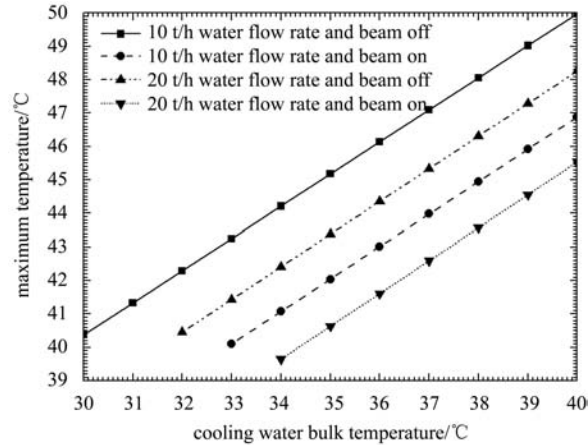


Fig. 12. The maximum temperature on the structure at different cooling water bulk temperatures.

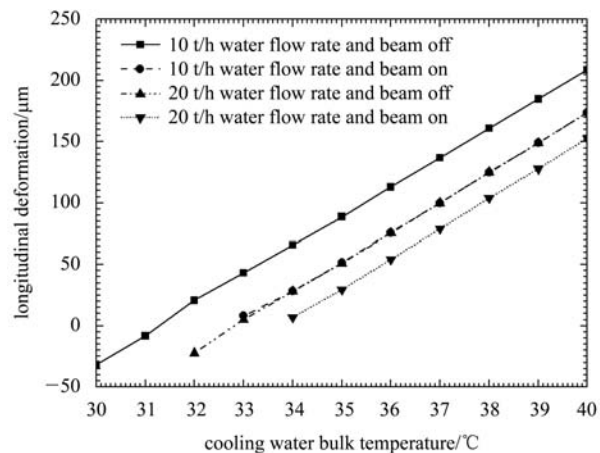


Fig. 13. The longitudinal deformation of the structure at different cooling water bulk temperatures.

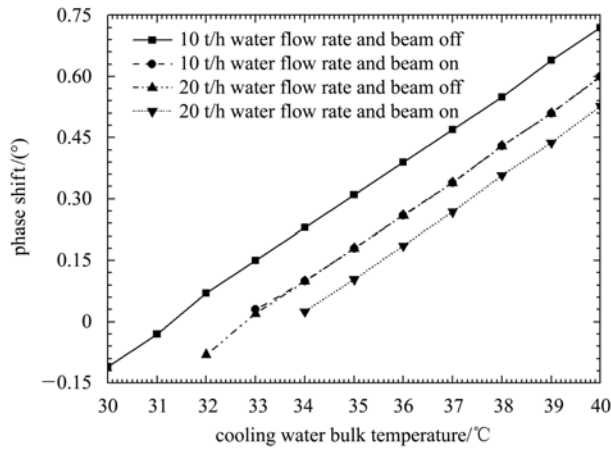


Fig. 14. The total phase shift of the electric field at different cooling water bulk temperatures.

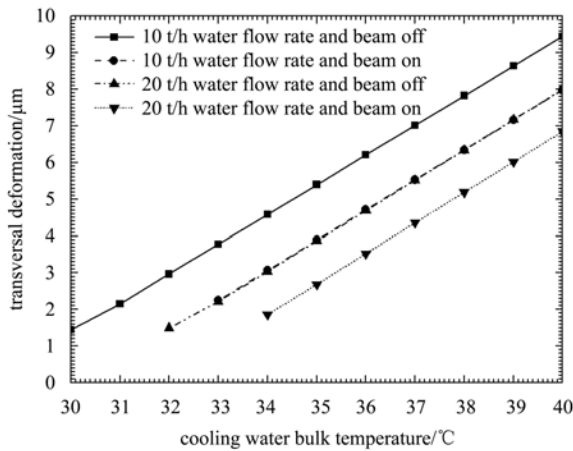


Fig. 15. The transversal deformation of the structure at different cooling water bulk temperatures.

the frequency shift by varying the cooling water temperature, and all the listed characteristics in the plots are linearly correlated with the cooling water bulk temperature. The optimized operating water temperature is  $\sim 32\text{ }^{\circ}\text{C}$ – $33\text{ }^{\circ}\text{C}$ .

To check the effect of water flow rate on the structure characteristic variations, calculations of a 20 t/h

water flow rate were also done, the results of which are also shown in Figs. 12 to 16. Compared with the 10 t/h case, its effect on the structure is a little bit smaller, there is  $\sim 2\text{ }^{\circ}\text{C}$  decrease of the maximum temperature rise. However, the cooling water system capability needs to be roughly doubled, so from a cooling power saving point of view, it is not very necessary.

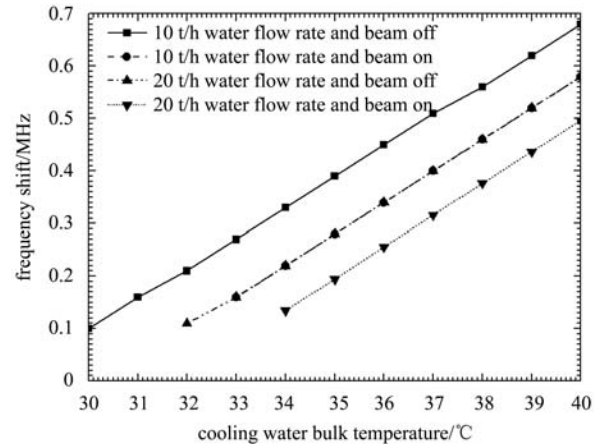


Fig. 16. The frequency shift of the structure at different cooling water bulk temperatures.

## 5 Conclusion

By replacing the real waveguide coupler with an axisymmetric on-axis coupled one in ANSYS, RF-thermal-structural-RF coupled analysis on the TW disk-loaded accelerating structure can be done with much less computer time and memory used.

The consistency between the simulation and experimental results of the BEPC II linac structure shows the validity of our simulation. The coupled analysis of the KIPT-linac structure shows that the optimized cooling water temperature is roughly  $\sim 32\text{ }^{\circ}\text{C}$ – $33\text{ }^{\circ}\text{C}$  and the RF heating caused frequency shift is fairly smaller than the structure's bandwidth, so a 10t/h water flow rate is enough for stable operation.

## References

- 1 The BEPC R & D Report, Part I, Injector, 1989
- 2 PEI Guo-Xi et al. Overview of BEPC II Linac Upgrade. Preliminary Design Report of BEPC II-Linac, IHEP-BEPC II-SB-03. 2002.6
- 3 ANSYS is a Trademark of SAS Inc., www.ansys.com
- 4 PEI Shi-Lun, CHI Yun-Long et al. Beam Dynamics Studies on the 100 MeV/100 kW Electron Linear Accelerator for NSC KIPT Neutron Source. Proceedings of IPAC2011. Spain: Kursall, San Sebastian, 2011. 9
- 5 CHI Yun-Long et al. Design Report on the NSC KIPT Electron Linear Accelerator. Version 2, IHEP, 2011.8
- 6 PEI Shi-Lun, WANG Shu-Hong. HEP & NP, 2005, **29**(9): 912–917 (in Chinese)
- 7 XU Zhao-Jun. Heat Transfer Theory. Beijing: China Machine Press, 1980. 57
- 8 YAO Chong-Guo. Electron Linear Accelerator. Beijing: Science Press, 1986
- 9 Billen J H, Young L M. Possion Superfish: LA-UR-96-1834. Los Alamos National Laboratory, 2002
- 10 The MAFIA collaboration. MAFIA User Manual (Version 4.106). Germany: CST Inc., 2000
- 11 SHU Zhao et al. High Power Laser and Particle Beams, 2011, **23**(1): 195–200 (in Chinese)